Spring 2018

Hydrodynamic Forces Acting on a Moving Hand

Elizabeth A. Gregorio

Hydrodynamic Forces Acting on a Moving Hand

Elizabeth A. Gregorio

An Honors Thesis
Submitted for partial fulfillment of the requirements for
graduation with honors in Physics from Hamline University

April 19th 2018

Abstract

The greatest amount of direct propulsion during swimming comes from the force exerted by the hand. It is possible for a swimmer to create a higher effective surface area of the hand by slightly spreading their fingers during the pull phase of the stroke. This phenomenon occurs because of the dynamic forces acting on the hand while it moves through the water. This investigation explores and compares how computational and experimental results suggest the occurrence of this phenomena. This is done first with a simple model of the four fingers (not including the thumb), held with different separations (0.0cm, 0.2cm, 0.3cm, 0.5cm, 1.0cm, 1.5cm) between them. Analysis is done using pressure differences, and drag force, and drag coefficients with ANSYS Fluent. These results are compared to values derived from experiments. Evidence of this phenomenon is found when small spacing is present during experiments in the water tank and confirmed by the computational results. This work is then extended to a study of a reconstructed 3D image of a hand. The effect the implementation of this technique during swimming is also considered.

Keywords: *Fluid Dynamics, Drag, Dynamic Pressure, Swimming.*

Contents

1 Introduction

When swimming freestyle, the largest portion of direct forward propulsion comes from the hand and forearm [2]. As the hand moves through the water, dynamic forces act on it. The contribution to propulsion stem from the lift force, drag force, and dynamic pressure distributions. These components in combination with the viscous nature of water allow for a swimmer to achieve a higher effective surface area of the hand when spreading the fingers.

Each of these components can be used to understand the forces contributing to propulsion in the different periods of the swimmer's stroke. The contribution from the lift force reaches its maximum when the thumb or fourth finger leads the motion of the hand [2]. This occurs during lateral skull movements such as those that happen for some swimmers during the catch phase of the stroke. The drag force reaches its maximum when the hand is oriented perpendicular to the direction of motion [2]. This is seen during the pull phase of the stroke. Pressure distributions can be used to understand the changes to the hydrodynamic characteristics when the fingers are spread [8]. The drag coefficient can be used to understand how hydrodynamic the shape is. A higher coefficient implies that the object has a shape that is less hydrodynamic.

This is seen in Figure 1, where all the objects have the same frontal area, but those with a less hydrodynamic shape have a larger drag coefficient [1]. The values presented in this figure were determined in a wind tunnel. The drag coefficients for these objects would be different in water, however, those with a larger value would continue to have a larger relative value.

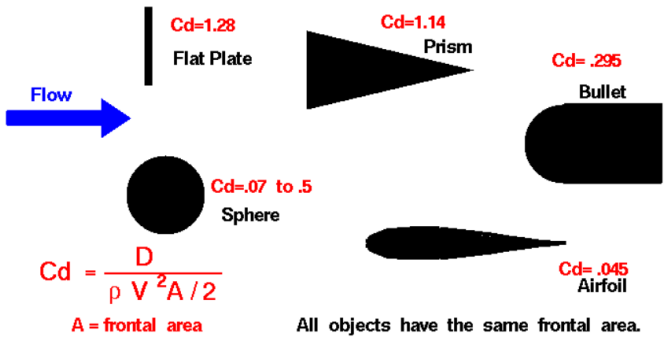

Figure 1: *Illustration of drag coefficients for shapes with varying hydrodynamic properties [1].*

This project aims to better understand the contribution this phenomenon has to the propulsion during the pull phase of the stroke. It especially aims to address the usefulness of spreading the fingers in relation to the amount of propulsive force produced. Therefore, the main tools of analysis will be the drag force and coefficient, and the dynamic pressure distributions.

The effective increase of surface area, hereafter referred to as the phenomenon, has been investigated using many different techniques. The main experimental methods include tow tanks such as in [2] and [7], or wind tunnels as seen in [4] and [8]. Computational methods have also been used, [3], [4], [5], [6]. Of these previous investigations the comparison between computational and experimental results has only been considered by Gardano, [4], using results obtained during experiments with human arm in the wind tunnel and computational results obtained with comparable conditions.

To expand on this prior research, experimental and computational methods will be employed. In this case the experiments are carried out in a water tank rather than a wind tunnel. Each of the experimental designs is created in such a way that a comparable computational analysis can be run. This is done with the goal of resolving the question of whether one method can predict the outcome of the other.

These methods are first employed for a simplified model of the hand, including the four fingers, (excluding the thumb). This model is specifically designed to resemble the separation between the fingers. The experiments are designed to obtain confirmation of the occurrence of this phenomena. Further, they aim to determine which spacings of the fingers for which the phenomenon is more effective.

Further experiments are designed for a three-dimensional reconstruction of a female human left hand. These are carried out using experimental methods in the water tank. With the intention of understanding how the original experiments can be extended to a hand. Additionally, the experiments allow for a better insight of the force per unit area of a swimmers hand when employing this phenomenon.

These results will then be utilized to analyze the possible usefulness of this phenomenon during competitive swimming. The largest spacing for which it occurs during experiments with the simplified model is used as a guideline to identify a bound for the amount of separation a swimmer can use. This separation is then used to identify the amount of added effective surface area a swimmer might achieve. This analysis in combination with that of the force per unit area of the hand allows for a better understanding of what this phenomenon can mean for the propulsion of the swimmer.

This paper is organized as follows. The models used during the experimental and computational trials are characterized in Section 2. The experimental and computational methods employed to obtain the results for the investigation are explained in Section 3. The calculations used to obtain the results from the physical trials are detailed in Section 4. The results of each of the methods are explained and displayed in Section 5. Conclusions of this study are presented and recommendations for use of this research are made in Section 6. Finally, the best avenues for further research on this topic are considered in Section 7.

2 Model Characterization

This section presents details about the creation of each of the models for use in experimental and computational trials.

2.1 Simplified Hand

The first observations were made with a simplified model of the human hand. This model is casted to resemble the spacing between the first four fingers, not including the thumb. The physical model created for experimental use is shown in the left image of Figure 2. The object is comprised of four slats connected with wire so that the spacing between them can be varied.

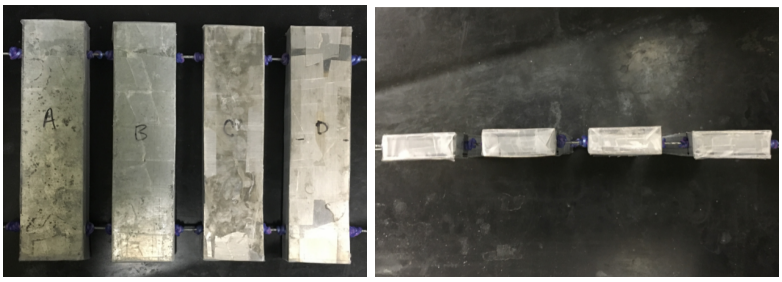

Figure 2: *Left: Over-head view of the four-finger model, Right: Side view of four finger model.*

This design was selected for a variety of reasons. The first of these is the movement of the water around this model needed to mimic the movement that would occur around a human hand. This means that when the amount of separation is increased the amount of surface area did not. This was accomplished as the same amount of wire is exposed when the slats are separated as when they are not. The edges of the slats also needed to have small enough edges for the shear force to be negligible. Finally, it was also selected for the ease of transferring it to a 2D computational model.

As can be seen in the right image of Figure 2 when looking at this model from the side, there are only four rectangles. This viewpoint for the model allowed for the creation of an identical computational model that could be investigated numerically in 2D. The version of this model used during computational trials can be seen in Figure 3.

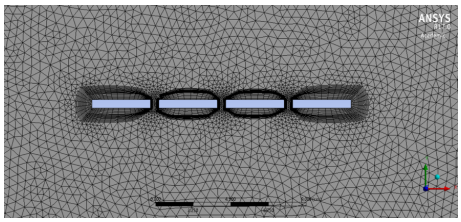

Figure 3: *A zoomed in view of the model and mesh created in ANSYS to replicate the physical model and used in numeric calculations.*

Figure 3 presents a view of the computational model that is as similar to the view in Figure 2 as possible. The meshing around the model is also visible. The numeric solution is found at each of the intersections of this mesh. The inflation around the object was created purposely so that more values would be found where there would be more movement.

2.2 3D Scan of Hand

A 3D model of a hand was also created to investigate how the results from the simplified model could be extended to an actual swimmer's hand. A scan was taken of the author's left hand first with fingers pressed together then again with small separation between the fingers. This was done with the Artec Spider 3D Scanner.

These scans were edited using Meshmixer to delete outliers, smooth irregularities, and remove artifacts resulting from the scanner's range of error. The 3D renderings of the edited hands can be seen in Figure 4.

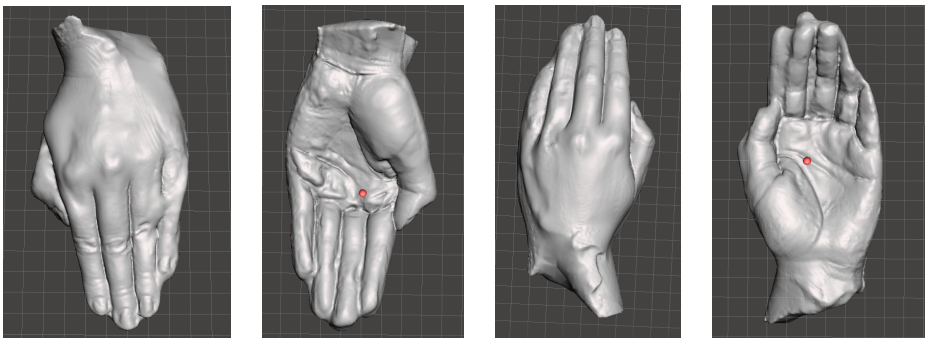

Figure 4: *Rendering of edited 3D scan of hand. Left to right: the left is the top view of no spacing, bottom view of no spacing, top view of small spacing, bottom view of small spacing.*

The quality of scans of the hands varies between the two. The scan with the fingers pressed together has very few irregularities from the author's actual hand. The scan of the hand with the fingers slightly separated has more artifacts. These are a result of the amount of detail that the scanner was able to translate. One of these artifacts is an actual webbing between the fingers for the scan taken with them held at a small spacing. The 3D editing and printing process could not be done with enough accuracy to remedy these artifacts and reproduce such a small separation between the fingers. For this reason the surface area of that hand is actually larger. Further experiments could be done after cutting spaces between these fingers.

3 Methods

This section explains the methods employed in order to obtain experimental and computational results for each of the models created.

3.1 Simplified Hand

The model of the four fingers was attached with string to a pulley system, for use in experimental trials. The other end of the string held a cup in which a mass could be placed for each experimental trial. A camera was set up directly across from the flat face of the water tank and black paper was attached to the far side of the tank to increase contrast. The full set up can be seen in Figure 5. This picture is taken from the same angle at which the camera was set.

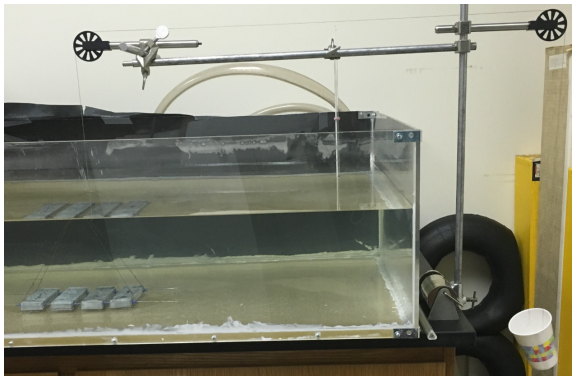

Figure 5: *Experimental setup for the simplified hand model.*

For each trial a 200g mass was placed in the cup, it was then allowed to fall freely, as the camera recorded the movement of the model. At least 24 falls were conducted for each spacing of the fingers. The average time to move to the surface and terminal velocity was determined from the recordings. This terminal velocity was used to dictate the speed of the fluid during the numeric solutions. An example of how the terminal velocity is identified can be found in Section 3.2, Figure 7.

3.2 3D Scan of Hand

The experimental set up for the reconstructed hand is similar to that of the "four finger" model. It can be seen in Figure 6. The model of the 3D reconstructed hand was printed using PLA (Polylactic Acid) filament in an Ultibox 2+. This hand was attached to a base constructed with foam-core. Two holes are cut on each face of the base so that it can be attached to the runners that span the top of the water tank. These runners are fashioned from PVC pipe. A string is attached to the front of the base of the hand, and connects it across a pulley, to a cup.

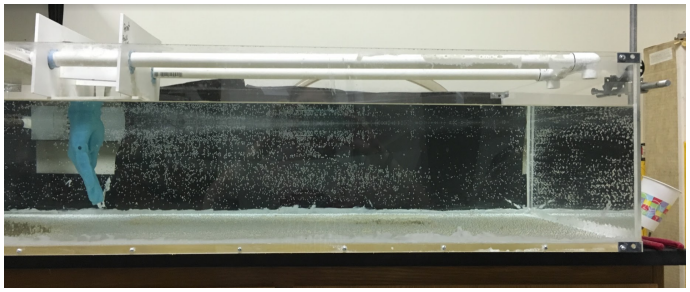

Figure 6: *Experimental setup for the 3D printed hand.*

A camera was placed across from the tank in the same position as described in Section 3.1, from which Figure 6 looks at the tank. Ten trials were run, during which a 277g mass was placed in the cup and allowed to fall freely. This procedure was followed for each of the two hands. The video recordings were analyzed, with Tracker, to identify the terminal velocity of the hand. An example plot of the hand's tracked movement across the tank can be seen in Figure 7.

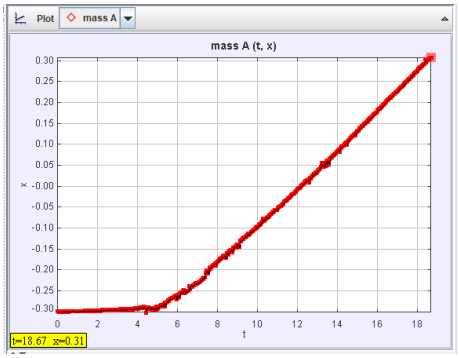

Figure 7: *Position (x) vs. time (t) example plot from Tracker.*

The plots such as the one shown in Figure 7 were used to determine at what point the hand reached terminal velocity. Terminal velocity can be identified by where the plotted line has constant slope and the least irregularities. In this case this includes the section of time between 15s and 18s. The program Tracker calculated the velocity in the x-direction throughout the video. An average of the velocities calculated in this range of time was taken to calculate the terminal velocity.

3.3 Percent Increase in Area

The amount of area that is added to the hand when the fingers are held at the most favorable spacing was also determined. To do this 2D scans were taken of subjects hands using a common copier. Subjects for the collection of this data volunteered to participate. Scans of 11 adult males and 12 adult females were obtained. Each of the images were collected by scanning the left and right hand of the subject. An example of a scan is presented in Figure 8. As seen in this example, these scans were taken with both hands placed on the glass with fingers pressed together. A ruler was included in each scan to judge relative lengths.

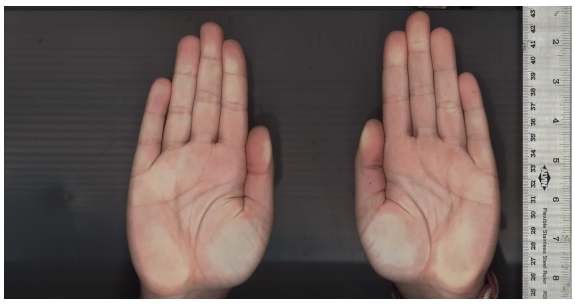

Figure 8: *Example of hand scans used to find the percent increase in area.*

These scans were printed for analysis. The length of the second, third, and fourth fingers was measured, and the area of the hands with fingers closed was estimated. Further details of these calculations are presented in Section 4.3.

4 Calculations

This section develops the equations necessary to find values of dynamic pressure, drag force and drag coefficient from the experimental results.

4.1 Pressure

The calculation of the expected dynamic pressure for each of the spacings was determined by the surface area for the model when all slats are pressed together. This area was used as a control for the calculations. The sum of the forces acting on this surface is as follows,

$$\sum F = F_T + F_B + F_{dP} - F_g \,. \tag{1}$$

Here, F_T is used for the force of tension, F_B is used for the force of buoyancy acting on the object, F_{dP} for the force from the dynamic pressure, and F_g for the force of gravity acting on the object. Where the force due to the difference in dynamic pressure is defined as,

$$F_{dP} = P_{dp} A \,. \tag{2}$$

Where A represents the actual surface area of the model, and P_{dp} represents the dynamic pressure.

Here we are only considering the portion during which the object reached its terminal velocity. Therefore, we are able to set Equation 1 to zero, substitute in Equation 2, and solve for P_{dp}. This gives,

$$P_{dp} = \frac{-F_T - F_B + F_g}{A} \,. \tag{3}$$

Sheer force calculations were performed with ANSYS and the values were deemed small enough to be negligible. For this reason they are ignored in this derivation.

The specifications of the model were used as input values for this equation to calculate the dynamic pressure for the experimental results section. The same equation was used to find the dynamic pressure for both the simplified four finger model and the 3D reconstructed hand.

4.2 Drag Force and Coefficient

To calculate the drag force, for the simplified four finger model, the following net force equation was derived in the same way as in Equation 2. The resulting equation is as follows,

$$\sum F = F_T + F_B - F_D - F_g \,. \tag{4}$$

Where, F_T is used for the force of tension, F_B is used for the force of buoyancy, F_D for the drag force, and F_g for the force of gravity. Again we are only considering the portion of movement for which the object displayed constant velocity allowing us to set the net force equal to zero and solve for the drag force as follows,

$$F_D = F_T + F_B - F_g \,. \tag{5}$$

This equation was then used to determine the value for drag force for the case of all fingers being held tightly together.

Due to the different experimental method for the 3D reconstruction of a hand, a different net force equation was required. It is derived as follows:

$$\sum F = F_g - F_{fr} - F_D \,. \tag{6}$$

Where F_{fr} represents the force of friction between the base of the hand and the runners, F_g is the gravitational force acting on the hanging mass, and F_D is the force of drag.

The portion of movement for which the hand reached its terminal velocity was selected again, allowing for F_D to be solved for as follows,

$$F_D = F_g - F_{fr}\,. \tag{7}$$

The value computed for the drag force was then used to find the drag coefficient with the following equation,

$$C_D = \frac{F_D}{\frac{1}{2} * \rho * A * v^2}\,. \tag{8}$$

Where A represents the surface area, v is the velocity of the model, and ρ is the density of water.

4.3 Area of Hand

An estimate of the surface area of the hand was obtained by measuring the length across the hand at specified intervals. A method similar to the trapezoidal method of integration in calculus was then used to obtain an estimate of the full area of the hand. The equation used for this purpose is,

$$A_o = \sum_i \frac{a_i + a_{i+1}}{2} h\,. \tag{9}$$

Where A_o represents the actual surface area of the hand, a_i is the first base of the hand and a_{i+1} is the next consecutive base, and h represents the length of the interval at which the hand was divided.

The space between each of the fingers is approximated to be a triangle with a base and a height. The base being the space between the fingers and the height being the length of the finger. In this case we are not considering the possible contribution from the abduction of the thumb from the palm. Therefore, the total added area is the sum of the contributions from the first, third, and fourth fingers as,

$$A_a = A_o + \frac{1}{2} b \sum (h_1 + h_3 + h_4) \,. \tag{10}$$

Where A_a is the amount of area added, b is the amount of space between the fingers, h_1 is the height of the first finger, h_2 is the height of the third finger, and h_4 is the height of the fourth finger.

The percent increase in the area of the hand was then calculated using the following equation:

$$Percent\ Increase = \frac{A_a - A_o}{A_o} * 100 \,. \tag{11}$$

Where the actual area of the hand with no consideration of possible increase to the effective surface area is used for A_o. The results for the percent increase in area are given in Sub-Section 5.3.

5 Results

This section presents interpretation and analysis for the data collected during the experimental and computational trials.

5.1 Simplified Hand

The time and velocity results of the experiments using the simplified hand model are shown in Table 1. By comparing the time to rise for each spacing we see that it takes significantly longer for the model to move through the water when held at 0.2cm spacing than any other tested spacing. The timing results for 0.30cm follows as the second longest to move through the water. This indicates that the model is indeed experiencing an increase in effective surface area during these trials.

Spacing (cm)	Time to Rise (s)	Velocity (cm/s)
0.01	1.307	16.162
0.20	1.395	13.214
0.30	1.353	14.027
0.50	1.311	13.724
1.00	1.246	18.915
1.50	1.193	16.148

Table 1: *Times and terminal velocities derived from videos of experimental trials.*

The values for the surface area of the object and the terminal velocity from the experiments were used to calculate pressure difference, drag force and coefficients displayed in 2. These values are presented alongside the results from the computations done in ANSYS Fluent with the same preconditions. Slight variations between the computational and experimental results are to be expected. Still, good agreement between the experimental and computational results should be present. This is taken into consideration during the discussion of results.

If the phenomenon is occurring, the effective surface area during the numeric solution would be larger than the actual surface area. The values calculated from the experimental values would not include this. All calculated results from the experiments only use values that are known with certainty. The actual surface area of the object is constant throughout these trials.

For this reason, the calculated drag force and pressure difference are the same for all spacings. The calculated drag coefficients differ across spacings because the terminal velocity of the object displayed in Table 1 is used.

	Calculated with ANSYS		Calculated from Experimental Results	
Spacing (cm)	Drag Force (N)	Drag Coefficient	Drag Force (N)	Drag Coefficient
0.01	-6.86433	-2.88889E-5	-1.1442	-4.63532
0.20	-0.13676	-8.59259E-7	-1.1442	-6.93428
0.30	-0.44151	-2.46667E-6	-1.1442	-6.15376
0.50	-1.40947	-8.22667E-6	-1.1442	-6.42849
1.00	-2.28252	-7.01333E-6	-1.1442	-3.38421
1.50	-1.82295	-7.68593E-6	-1.1442	-4.64336
Spacing (cm)	Pressure Difference (Pa)		Pressure Difference (Pa)	
0.01	51.75		60.05	
0.20	39.87		60.05	
0.30	58.24		60.05	
0.50	61.02		60.05	
1.00	64.41		60.05	
1.50	68.07		60.05	

Table 2: *Comparison of calculated pressures and drag.*

Good agreement can be seen between the computational and experimental values for the drag force and dynamic pressure. However, the values drag coefficients are significantly different between the two methods and the cause of this difference is unknown. The other two methods of analysis can still be used to compare the trials.

When inspecting the drag force, it is evident that the values for the smaller spacings are larger than the others. The 0.20cm spacing has a significantly larger amount of drag force at -0.13676N. The next closest amount of drag force is calculated for the 0.30cm spacing which has -0.44151N. These values mirror the experimental results displayed in Table 1 where the 0.20cm and 0.30cm spacings took the longest period of time to travel through the water.

The values for drag coefficients can be considered separately for the computational values and experimental values. The negative signs for these values are due to the direction of fluid flow. Reviewing the data collected for the coefficients we see that the calculated coefficients are smallest for the smaller spacings. In this case these spacings include the 0.20cm, 0.30cm, and 0.50cm spacings. This observation again carries over to the results calculated during the computational trials, where the smallest drag coefficients are reported to be for the same small spacings of the fingers. This trend is opposite of what would be expected based on the theory presented in Section 1. Further investigations would be required to determine the reason for the difference in

values between the computational and experimental methods, and the reason for this difference from theory.

The results for pressure differentials found during numerical trials have similar values to what was expected. The large differences between the values for the pressure at each spacing can most likely be attributed to the different values for pressure used during these calculations. However, it is unusual that the pressure difference increases as the spacing increases. The pressure contours for these calculations are shown in Figure 9. These are the pressure contours calculated around the 2D simplified model. The object is in the center of these images, and can be seen with more detail earlier in this paper in Figure 3.

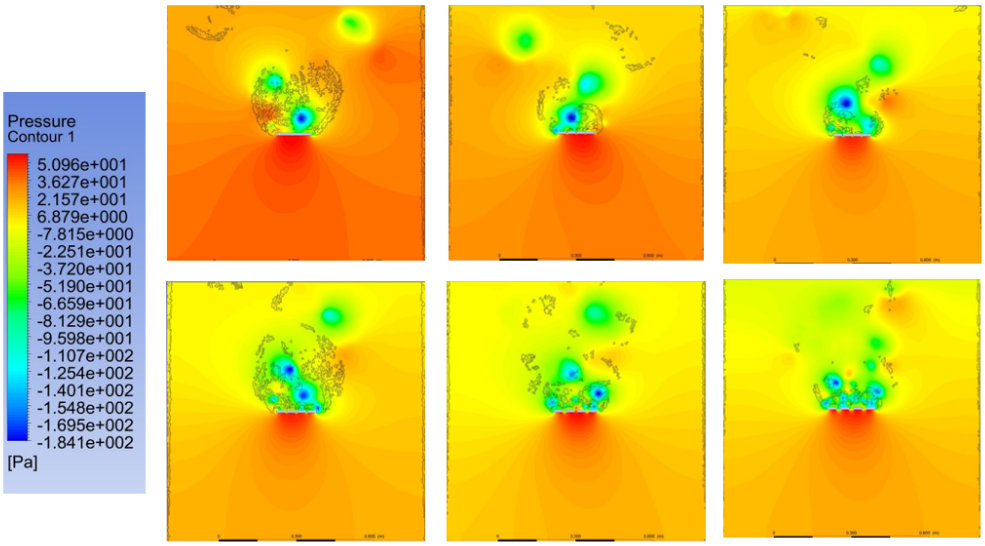

Figure 9: *Pressure contours for the numeric solutions.*

In Figure 9 the first pressure contour shown in the top left is for the 0.01cm spacing, and the bottom left is 0.5cm. The spacings increase as you move to the right in both rows. In the computational trials the inlet for the fluid was dictated to be the bottom edge of the computational field. This means that the water is entering along the bottom edge of these pressure contours. Keeping this in mind we can analyze the pressure contours displayed in Figure 9.

By inspecting the pressure contours in Figure 9 it is apparent that even though the output values are larger for the larger spacings, the pressure distributions decrease as the spacing increases. Further, showing that these values are a result of the differing input velocities. Still these results to not provide any indication as to which spacing is the most effective for increasing the effective surface area of the hand.

The cumulative evidence from these methods of analysis indicate that the phenomenon is occurring during these experiments. Additionally, we see that the computational and experimental methods produce similar results, so that one method would be able to predict the results of the other. Further, the results indicate that the largest spacing for which it is possible for the phenomena to occur is 0.50cm. While the most effective spacing for this use is 0.20cm.

5.2 3D Scan of Hand

The results from the experiments with the 3D printed hand are presented in Table 3. The data presented for the actual surface area of the hand, (A_o), were calculated using the experimental results obtained with the use of the 3D scan of a hand with no spacing between the fingers. Those displayed for the increased area, (A_a), were calculated with the experimental results from the model of the hand with small separation between the fingers. Recall that the hand with the small spacing between the fingers actually has a larger surface area due to artifacts of the scan.

The values for the surface area of the hand presented in Table 3 were found for the author's left hand using a the 2D scan in Figure 8. The actual surface area that is exerting force on the water for the 3D reconstruction of the hand is different because this scan was taken with the curvature in the hand that would be present when swimming. These results are can therefore be considered only as an estimation.

	Surface Area	Average Velocity	Drag Force	Drag Coefficient	Pressure Difference
Actual Area (A_o)	128.32 cm^2	0.047 m/s	1.11 N	77.61	86.50 Pa
Increased Area (A_a)	131.49 cm^2	0.038 m/s	1.11 N	115.87	83.87 Pa

Table 3: *Results from the experiments and calculations for the 3D printed hand.*

The velocity for the hand with spacing between the fingers experiences a slower velocity than the hand with fingers pressed together. This follows the trend shown in Table 1. Although there is no actual space between the fingers for the 3D hand, this comparison allows for an inference that a similar result would be attained if there were. Specifically, similar results would be expected for a swimmer employing this technique, with actual separation of their fingers, during competition.

The drag forces presented are the same for each of these spacings. This is the case because they were both subjected to the same gravitational force acting on the free hanging mass and frictional force as seen in Equation 7. By keeping these constant the only differences between the hands in the force and pressure analysis could be the drag coefficient and pressure difference.

The drag coefficient for the hand with spacing between the fingers is larger than that of the other model. This again follows from the calculated results for the simplified hand presented in Table 2. The pressure difference also decreases as expected. Further experiments with a model with actual separation between the fingers would be required to be able to confirm these comparisons.

5.3 Percent Area Increase

These results were calculated using the 2D scans and the equations derived in Section 4.3. The results from Section 5.1 were used to determine the spacing which would be used to estimate the increase in surface area for a swimmer's hand. It was decided that using a spacing closer to the most effective spacing would best indicate the potential for this technique. Therefore, the results presented here were calculated with an assumed 0.03cm separation between the four fingers where appropriate.

The results presented here are estimations. The actual the surface area of a hand that applies force to the water would not be the full surface area of the hand. The curvature of the hand that is used in swimming was not accounted for in these calculations.

The two dimensional scans of eleven males and twelve female adults were obtained and measured. These measurements were used to calculate the surface area of the hand as well as the amount of surface area could be added if this phenomena occurs perfectly with a 0.3cm separation between the four fingers. The results from these calculations are displayed in Table 4. These results represent the combined increase and percent increase in surface area for both the left and right hand.

		Male	Female
Area Increase	Average (cm^2)	6.35	5.93
	Maximum (cm^2)	7.12	6.84
	Minimum (cm^2)	5.95	5.28
Percent Increase	Average (%)	2.38	2.53
	Maximum (%)	2.67	2.94
	Minimum (%)	2.08	2.26

Table 4: *Results of hand surface area calculations.*

These calculations show that the surface area of the hand is increased by about $3cm^2$ per hand when the phenomena works perfectly. This represents less than a 3% increase in surface area. These results represent the amount of increased area a swimmer might expect for their flat hand with a 0.30cm spacing.

The results for the amount of force applied by the hand found in Section 5.2 were applied to the calculated increased surface areas. This was done to calculate the amount of propulsive force generated with the actual surface area of the hand as well as the increased area. The results of these calculations can be found in 5. These results represent the combined force and pressure difference for both the left and right hand.

		Male	Female
Actual Area	Pressure (Pa)	82.67	93.60
	Drag Force (N)	2.22	2.22
	Drag Coefficient	74.15	83.95
Increased Area	Pressure (Pa)	80.76	91.69
	Drag Force (N)	2.22	2.22
	Drag Coefficient	111.85	127.00

Table 5: *Estimations for the amount of force a hand would be able to apply with the actual surface area and the increased surface area.*

The results presented in Table 5 are calculated using a combination of results from previous sections. Determining these values required the average actual and increased surface areas as well as the average velocity and drag force determined during experiments. These results are a preliminary example of how much force could be generated. However, further experiments

with a model that has real separation between the fingers would be required to check these results. These values can be found in Table 4 and in the previous section in Table 3 respectively.

These values should only be compared within the female and male categories. The pressure decreases as the surface area increases, while, the drag coefficients increase as the surface area increases. Both of these results are as expected based on the theory.

All of these results follow closely with the results for the simplified model and those derived directly from the experiment. This reinforces the idea that any of these methods can be used to predict the results of another.

6 Conclusions

The results presented in this paper suggest that there is an effective increase in surface area of a swimmers hand if they were to slightly separate their fingers. This is inferred from the trials using the simplified model, where in experiments it took a longer amount of time for the model to move through the water. This effective increase was also seen during the numeric results where the small spacings experienced a larger amount of drag force.

These results can be used to understand how useful this technique would be for a competitive swimmer. From the percent increase in area analysis, it is apparent that employing this practice with a 0.30cm separation between the fingers may allow for less than a 3% increase in surface area for both male and female swimmers. In both cases we see a increase in drag coefficient for the experiments done with the hand with the larger surface area. However, further experiments would be required to confirm these results.

Another factor to consider when determining the usefulness of this technique for a competitive swimmer is the ease of holding the fingers at this specific separation while swimming. Although it is possible to increase ones effective surface area holding the fingers at this separation it might be difficult to ensure that the fingers do not slip. If this were to happen and the fingers were to end up at a much larger separation than that recommended here, we see from the results of the simplified hand model, that the fingers being farther apart is actually less effective than having them be pressed together. Therefore, the ability of the swimmer to hold their fingers at this specific separation during a race must also be taken into consideration before employing this technique in competition.

7 Future Directions

The work done in this investigation has begun the process of determining the usefulness of this phenomenon for competitive swimmers. However, the topic should be further explored.

In this work it was not possible to attain realistic conditions with experiments. The velocities at which both models of the hand move are significantly slower than would be true for an actual swimmers hand. However, this investigation was successful in showing that the numerical solutions are predictive of experimental results. Therefore, these or similar calculations can be run at a more realistic speed for a swimmer's hand without further experiments being necessary.

Numeric solutions could also be attained for the 3D model of a human hand at different spacing. The 3D scanner and reconstruction methods used here were unable to produce a hand with real space between the fingers. Therefore, continuing the data collection in this area could allow for a better understanding of this phenomenon.

It would also be useful to conduct the experiments with the 3D reconstructed hand for a model with actual separation between the fingers. It would also be useful to run numeric simulations with such a model. This might allow for a better estimate of the surface area of the hand which applies force during the pull phase.

8 Acknowledgements

Kevin Stanley for being my research advisor and mentor. Earl E. Bakken Medical Devices Center for granting me free access to the Artec Spider 3D Scanner for use in this project. Jesse Erickson for setting up ANSYS on the VDI network, and providing technical support whenever needed. Josiah Biernat and Rutger Krenz for building the water tank. The physics faculty for their support, and to the department for funding my project.

References

[1] National Aeronautics and Space Administration. Shape effects on drag, 2015.

[2] Monique A.M. Berger, Gert de Groot, and A. Peter Hollander. Hydrodynamic drag and lift forces on human hand/arm models. *Journal of Biomechanics*, 28(2):125–133, 1995.

[3] Milda Bilinauskaite, Vishveshwar Rajendra Mantha, Abel Ilah Rouboa, Pranas Ziliukas, and Antonio Jose Silva. Computational fluid dynamics study of swimmer's hand velocity, orientation, and shape: contributions to hydrodynamics. *BioMed Research International*, 2013.

[4] Paola Gardano and Peter Dabnichki. On hydrodynamics of drag and lift of the human arm. *Journal of Biomechanics*, 39(15):2767–2773, 2006.

[5] Daniel A. Marinho, Tiago M. Barbosa, Victor M. Reis, Per L. Kjendlie, Francisco B. Alves, Joao P. Vilas-Boas, Leandro Machado, António J. Silva, and Abel I. Rouboa. Swimming propulsion forces are enhanced by a small finger spread. *Journal of applied biomechanics*, 26(1):87–92, 2010.

[6] Daniel A. Marinho, Abel I. Rouboa, Francisco B. Alves, João P. Vilas-Boas, Leandro Machado, Victor M. Reis, and António J. Silva. Hydrodynamic analysis of different thumb positions in swimming. *Journal of Sports Science and Medicine*, 8(1):58–66, 2009.

[7] N.O. Sidelnik and B.W. Young. Optimising the freestyle swimming stroke: the effect of finger spread. *Sports Engineering*, 9(3):129–135, 2006.

[8] Hideki Takagi, Yukimaru Shimizu, Akihiro Kurashima, and Ross Sanders. Effect of thumb abduction and adduction on hydrodynamic characteristics of a model of the human hand. 2001.